Published in final edited form as:
Liver Int. 2010 May ; 30(5): 669–682. doi:10.1111/j.1478-3231.2010.02205.x.

Hypoxia Stimulates Hepatocyte Epithelial to Mesenchymal Transition by Hypoxiainducible Factor- and Transforming Growth Factor-β-dependent Mechanisms

Bryan L. Copple
Department of Pharmacology, Toxicology, and Experimental Therapeutics University of Kansas Medical Center, Kansas City, KS 66160

Abstract

Background/Aims—During development of liver fibrosis, an important source of myofibroblasts is hepatocytes, which differentiate into myofibroblasts by epithelial to mesenchymal transition (EMT). In epithelial tumors and kidney fibrosis, hypoxia, through activation of hypoxia-inducible factors (HIFs), is an important stimulus of EMT. Our recent studies demonstrated that HIF-1α is important for the development of liver fibrosis. Accordingly, the hypothesis was tested that hypoxia stimulates hepatocyte EMT by a HIF-dependent mechanism.

Methods—Primary mouse hepatocytes were exposed to room air or 1% oxygen and EMT evaluated. In addition, bile duct ligations (BDLs) were performed in Control and HIF-1α-deficient mice and EMT quantified.

Results—Exposure of hepatocytes to 1% oxygen increased expression of α-smooth muscle actin, vimentin, Snail, and fibroblast-specific protein-1 (FSP-1). Levels of E-cadherin and zona occludens-1 were decreased. Upregulation of FSP-1 and Snail by hypoxia was completely prevented in HIF-1β-deficient hepatocytes and by pretreatment with SB431542, a TGF-β receptor inhibitor. HIFs promoted TGF-β-dependent EMT by stimulating activation of latent TGF-β1. To determine whether HIF-1α contributes to EMT in the liver during the development of fibrosis, Control and HIF-1α-deficient mice were subjected to BDL. FSP-1 was increased to a greater extent in the livers of Control mice when compared to HIF-1α-deficient mice.

Conclusions—Results from these studies demonstrate that hypoxia stimulates hepatocyte EMT by a HIF and TGF-β-dependent mechanism. Furthermore, these studies suggest that HIF-1α is important for EMT in the liver during the development of fibrosis.

Keywords

hepatocyte; hypoxia-inducible factors; epithelial to mesenchymal transition; transforming growth factor-β; fibroblast-specific protein-1; Snail

Liver fibrosis is characterized by excessive deposition of extracellular matrix in the liver during chronic injury. This disease is initiated when liver injury stimulates cells in the liver to synthesize and secrete proteins and other soluble mediators that, in turn, stimulate cells, such as hepatic stellate cells (HSCs) and peribiliary fibroblasts to differentiate into myofibroblasts and produce collagen (1). In addition to these cells types, recent studies have

Contact Information for Corresponding Author: Bryan L. Copple, Ph.D. Department of Pharmacology, Toxicology, and Therapeutics University of Kansas Medical Center 4063 KLSIC 3901 Rainbow Boulevard Kansas City, KS 66160 Phone: (913)588-7142 Fax: (913)588-7501 bcopple@kumc.edu.

demonstrated that hepatocytes and bile duct epithelial cells also differentiate into fibroblasts by a process termed epithelial to mesenchymal transition (EMT) (2, 3).

Recent studies from our laboratory demonstrated that hypoxia, through activation of the transcription factor, hypoxia-inducible factor-1α (HIF-1α), is an important driving force for the development of liver fibrosis (4). In these studies, mice deficient in HIF-1α had reduced collagen deposition and fewer activated fibroblasts in the liver when subjected to bile duct ligation, a commonly used animal model of liver fibrosis (4). These results suggested that HIF-1α is a key mediator of fibrosis in the liver during chronic injury. What remained unclear from these studies, however, was the molecular mechanism by which HIF-1α promoted fibrosis.

Recent studies in the kidney demonstrated that HIF-1α promotes kidney fibrosis by stimulating conversion of renal epithelial cells to a mesenchymal cell phenotype by EMT (5). During EMT, levels of epithelial cell-specific proteins are decreased, such as zona occludens-1 and E-cadherin, and levels of mesenchymal cell-specific proteins are increased, such as α-smooth muscle actin (α-SMA), vimentin, and collagen (6). EMT has long been recognized as a process important for normal embryonic development, tumor cell metastasis, and kidney and liver fibrosis (3, 5, 6). Hepatocytes and bile duct epithelial cells can transdifferentiate into mesenchymal cells by EMT and deposit collagen in the liver during chronic injury. Although studies have established that hepatocyte EMT contributes to the development of fibrosis, whether hypoxia, through activation of HIF-1α, is a stimulus for hepatocyte EMT is not known. Since HIF-1α is important for the development of fibrosis and HIF-1α stimulates EMT in kidney and tumors, it is possible that HIF-1α may promote liver fibrosis in part by stimulating hepatocyte EMT. Accordingly, in the present study, the hypothesis was tested that hypoxia stimulates hepatocyte EMT by a HIF-dependent mechanism.

Materials and methods

Mice

C57BL/6 mice (Harlan, Madison, WI), HIF-1α-control mice, HIF-1α-deficient mice, HIF-1β-control mice, and HIF-1β-deficient mice were used for all studies. Generation of the HIF-1α-control mice, HIF-1α-deficient mice, HIF-1β-control mice, and HIF-1β-deficient mice was described previously (7–9). Mice were maintained on a 12-h light/dark cycle under controlled temperature (18–21°C) and humidity. Food (Rodent Chow; Harlan-Teklad, Madison, WI) and tap water were allowed ad libitum. All procedures on animals were carried out in accordance with the Guide for the Care and Use of Laboratory Animals promulgated by the National Institutes of Health and were approved by the institutional IACUC committee at the University of Kansas Medical Center.

Hepatocyte Isolation

Hepatocytes were isolated from the livers of mice by collagenase perfusion as described previously, and cultured in room air or 1% oxygen in a NAPCO CO_2 7000 cell culture incubator (NAPCO Precision, Winchester, VA) (7). These environments also contained 5% CO_2 and were balanced with nitrogen. The hepatocytes were cultured on collagen-coated 6 well plates in Williams' Medium E supplemented with 10% FBS and Penicillin-Streptomycin. After a 3 hour attachment period, the medium with unattached cells was removed, and the cultures washed with 1× phosphate-buffered saline. Fresh serum-free Williams' medium E with antibiotics was then added and the cells cultured for 16 hours before exposure to hypoxia. The viability of the isolated hepatocytes was >85% by the criterion of trypan blue (Sigma Chemical Company) exclusion. The cultures contained 2.3

+/− 0.8 % hepatic stellate cells, 1.9 +/− 1.0 % Kupffer cells, and 2.4 +/− 1.1 % endothelial cells as determined by immunostaining for glial fibrillary acidic protein (GFAP), F4/80, and mouse endothelial cell antigen-32 (MECA-32) respectively.

Hepatic Stellate Cell (HSC) Isolation

HSCs were isolated from mice by dual perfusion with collagenase and pronase as described in detail previously (10). The cells were cultured on collagen-coated 6 well plates in Williams' medium E supplemented with 10% FBS and penicillin-streptomycin. After 4 hours, the cells were washed with PBS and the medium replaced with serum-free Williams' medium E containing antibiotics. The cells were cultured for 16 hours and then placed in room air or 1% oxygen as described above. These conditions were chosen to mimic the hepatocyte culture conditions.

Real-time PCR

Real-time PCR was performed as described previously (11). The sequences of the primers were as follows: 18S Forward: 5'-TTGACGGAAGGGCACCACCAG-3'; 18S Reverse: 5'-GCACCACCACCCACGGAATCG-3'; Vimentin Forward: 5'-CGGAAAGTGGAATCCTTGCA-3'; Vimentin Reverse: 5'-CACATCGATCTGGACATGCTGT-3'; Slug Forward: 5'-TGATGCCCAGTCTAGGAAATCG-3'; Slug Reverse: 5'-GCCACAGATCTTGCAGACACAA-3'; TWIST Forward: 5'-CCCCACTTTTTGACGAAGAATG-3'; TWIST Reverse: 5'-AAAATGGAGCCAGTCACATGTGG-3'; α-SMA Forward: 5'-CCACCGCAAATGCTTCTAAGT-3'; α-SMA Reverse: 5'-GGCAGGAATGATTTGGAAAGG-3'; FSP-1 Forward: 5'-GAAGCTGCATTCCAGAAGGTGA-3'; FSP-1 Reverse: 5'-CATCATGGCAATGCAGGACA-3'; Snail Forward: 5'TTTTGCTGACCGCTCCAAC-3'; Snail Reverse: 5'-TGCTTGTGGAG AAGGACAT-3'; Glut1 Forward 5'-TCGGCCTCTTTGTTAATCGCT-3'; Glut1 Reverse 5'-GGACTTGCCCAGTTTGGAGAA-3'; TGF-β1 Forward: 5'-TGCTAATGGTGGACCGCAA-3'; TGF-β1 Reverse: 5'-CACTGCTTCCCGAATGTCTGA-3'; TGF-β2 Forward: 5'-TAATTGCTGCCTTCGCCCT-3'; TGF-β2 Reverse: 5'- CCCCAGCACAGAAGTTAGCATT-3'; TGF-β3 Forward: 5'-CACCAATTACTGCTTCCGCAA -3'; TGF-β3 Reverse: 5'-TAGGTTCGTGGACCC TTTCC -3'.

Western Blot Analysis

Nuclear extracts were isolated from hepatocytes and western blotting performed as described previously (7). Snail was detected using a rabbit anti-Snail antibody (Abcam, Cambridge, MA). HIFs were detected with either rabbit polyclonal anti-HIF-1α antibody (NB100-449, Novus Biologicals, Littleton, CO) diluted 1:1000 or rabbit polyclonal anti-HIF-2α (NB100-122, Novus BIologicals) diluted 1:1000, followed by incubation with goat anti-rabbit antibody conjugated to horseradish peroxidase (Santa Cruz Biotechnology). Immunoreactive bands were visualized using the Immun-Star HRP Substrate Kit (Bio-Rad Laboratories, Hercules CA).

Immunocytochemistry

Hepatocytes were fixed in 4% formalin, and then blocked with phosphate-buffered saline containing 3% goat serum. The cells were incubated with rabbit anti-Snail antibody (catalog number: ab17732, Abcam), rabbit anti-E-cadherin antibody (catalog number: 3195, Cell Signaling Inc.), rabbit anti-zona occludens-1 (catalog number: 402300, Invitrogen), mouse

anti-vimentin antibody (catalog number: 40E-C, Developmental Studies Hybridoma Bank, Iowa City, IA), rat anti-mouse endothelial cell antigen (catalog number: MECA-32, Developmental Studies Hybridoma Bank), rat anti-F4/80 (catalog number: MCA497, Serotec), chicken anti-GFAP (catalog number: ab4674, Abcam, Cambridge, MA), or rabbit polyclonal anti-FSP-1 antibody (catalog number: ab27957, Abcam) followed by incubation with secondary antibody conjugated to either Alexa 488 or Alexa 594 (Molecular Probes, Eugene, OR). For staining of F-actin, cells were incubated with phalloidin-labeled with Alexa 594 as per manufacturer's recommendation (Molecular Probes). For all immunocytochemistry, no fluorescence was observed in the absence of primary antibody.

Immunohistochemistry

For FSP-1, albumin, and cytokeratin-19 (CK19) immunostaining, livers were frozen in isopentane (Sigma Chemical Company) immersed in liquid nitrogen for 8 minutes. Sections of frozen liver were fixed in 4% formalin in phosphate-buffered saline (PBS) for 10 min at room temperature. Sections were incubated with rabbit polyclonal anti-FSP-1 antibody (catalog number: ab27957, Abcam), goat anti-mouse serum albumin (catalog number: ab19194, Abcam), or rat anti-CK19 (catalog number: TROMA-III, Developmental Studies Hybridoma Bank) diluted 1:50 in PBS containing 3% goat serum at room temperature for 3 h. The sections were washed with PBS, and then incubated with secondary antibody conjugated to Alexa 594 (FSP-1) or Alexa 488 (CK-19 or albumin). Colocalization of FSP-1 immunostaining with CK-19 or albumin immunostaining was observed on a Nikon confocal microscope. Total FSP-1 immunostaining in the liver was quantified morphometrically by analyzing the area of immunohistochemical staining of FSP-1 in a section of liver using Scion Image software (Scion Corporation, Frederick, MD) as described (12). The staining is expressed as a fraction of the total area. The random fields analyzed for each liver section were averaged and counted as a replicate, i.e., each replicate represents a different mouse. Peribiliary FSP-1 staining was quantified by measuring the area of FSP-1 staining that occurred within 100 μm of CK-19 staining. Nonperibiliary FSP-1 staining was determined by subtracting peribiliary FSP-1 staining from the total FSP-1 staining. For all immunohistochemistry, no fluorescence was observed in the absence of primary antibody.

Quantification of TGF-β1

Total and active TGF-β1 were measured using a commercially available kit (R&D Systems) as per manufacturers' recommendations.

Bile Duct Ligation

HIF-1α-control mice and HIF-1α-deficient mice 8–12 weeks of age were anesthetized with isoflurane. A midline laparotomy was performed and the bile duct ligated with 3-0 surgical silk. The abdominal incision was closed with sutures, and the mice received 0.2 mg/kg Buprenex by subcutaneous injection.

Statistics

Results are presented as the mean ± SEM. Data were analyzed by Analysis of Variance (ANOVA). Comparisons among group means were made using the Student-Newman-Keuls test. The criterion for significance was $p < 0.05$ for all studies.

Results

Hypoxia Increases Expression of EMT Genes in Primary Mouse Hepatocytes

Exposure of primary mouse hepatocytes to 1% oxygen caused an increase in mRNA levels of the EMT genes, FSP-1, α-SMA, and vimentin (Fig. 1) (6). In addition, exposure of

hepatocytes to hypoxia increased levels of Snail mRNA (Fig. 2A) and protein (Fig. 2B and 2D). Levels of two other EMT transcription factors, Slug and TWIST, were unaffected in hypoxic hepatocytes (Fig. 2E and 2F). To rule out the possibility that the observed increases in these genes was due to hepatic stellate cell contamination of the hepatocyte cultures, hepatic stellate cells were isolated from mice and exposed to room air or 1% oxygen for 3 days. Exposure of hepatic stellate cells to 1% oxygen for 3 days did not increase levels of α-SMA, FSP-1, or Snail mRNAs when compared to hepatic stellate cells exposed to room air for 3 days (Fig. 3). This indicated that the increases in α-SMA, FSP-1 and Snail observed in hypoxic hepatocytes were not due to contamination by hepatic stellate cells.

Decreased Levels of the Epithelial Proteins, E-cadherin and Zona Occludens-1, in Hypoxic Hepatocytes

In cultures of hepatocytes incubated in room air, E-cadherin immunostaining was observed at the cell surface of most of hepatocytes in culture (Fig. 4A). In hepatocytes cultured in 1% oxygen, E-cadherin immunostaining at the cell surface of hepatocytes was largely absent (Fig. 4B). Similarly, zona occludens immunostaining was observed on the outer cell membrane of hepatocytes cultured in room air (Fig. 4C). In hepatocytes cultured in 1% oxygen, minimal zona occludens-1 immunostaining was observed (Fig. 4D). In many of the hypoxic cells, zona occludens-1 was observed within the cell indicating that it had been internalized.

Reorganization of the Actin Cytoskeleton and Morphological Changes in Hypoxic Hepatocytes

During EMT, cytoskeletal proteins, such as F-actin, become reorganized into stress fibers (13). To observe this in hypoxic hepatocytes, the cells were stained with fluorescently-labeled phalloidin. In hepatocytes cultured in room air, F-actin was primarily organized around the plasma membrane of the cell (Fig. 4E). F-actin within the cytoplasm of these cells remained unorganized. In hypoxic hepatocytes, F-actin was highly organized into fibers that extended from the cell surface through the cytoplasm (Fig. 4F). In addition, stress fibers were observed in the hepatocytes cultured in hypoxia (Fig. 4F).

Consistent with hypoxia stimulating hepatocyte EMT, hepatocytes cultured in hypoxia were morphologically similar to fibroblasts with numerous projections and pseudopodia (Fig. 5B).

Increased Levels of Vimentin and FSP-1 Proteins in Hypoxic Hepatocytes

Positive immunostaining for vimentin (Fig. 5C) and FSP-1 (Fig. 5E) was largely absent in cultures of hepatocytes exposed to room air. In hepatocytes exposed to 1% oxygen, vimentin (Fig. 5D) and FSP-1 (Fig. 5F) immunostaining was observed in nearly all cells.

Hypoxia-inducible Factors are Required for Hypoxia-induced EMT in Hepatocytes

Next, we determined whether hypoxia-induced EMT required HIFs. Exposure of hepatocytes isolated from HIF-1β-control mice, which have normal levels of HIF-1β, to 1% oxygen increased mRNA levels of Glut-1 (a known HIF target gene), FSP-1, Snail, and α-SMA (Fig. 6A–6D). Upregulation of all of these genes was completely prevented in hepatocytes isolated from HIF-1β-deficient mice, which are deficient in both HIF-1α and HIF-2α signaling (Fig. 6A–6D) (14, 15).

Role of TGF-β signaling in hypoxia-induced EMT in hepatocytes

TGF-β1 is a known, potent stimulator of hepatocyte EMT (3). Therefore, we next determined whether hypoxia-induced hepatocyte EMT required TGF-β signaling. To inhibit

TGF-β signaling, hepatocytes were preincubated with the TGF-β type I receptor inhibitor, SB-431542 (16). Hypoxia increased mRNA levels of FSP-1 and Snail in vehicle-treated hepatocytes exposed to 1% oxygen (Fig. 7A and 7B). Similarly, TGF-β1 increased FSP-1 and Snail mRNA levels in vehicle-treated hepatocytes (Fig. 7A and 7B). Upregulation of both FSP-1 and Snail by either 1% oxygen or TGF-β1 was completely prevented by pretreatment with SB-431542 (Fig. 7A and 7B). Upregulation of glucose transporter-1 by hypoxia in hepatocytes was unaffected by pretreatment with SB-431542 (Fig. 7C). This demonstrates that SB-431542 did not prevent upregulation of all HIF-regulated genes in hypoxic hepatocytes, and that the effect was specific to EMT genes. Furthermore, TGF-β1 did not increase glucose transporter-1 mRNA levels, suggesting that TGF-β signaling occurred downstream of HIF activation (Fig. 7C). Consistent with this observation, SB-431542 did not prevent activation of either HIF-1α (Fig. 8A) or HIF-2α (Fig. 8B) in hypoxic hepatocytes. Similarly, TGF-β1 did not activate either HIF-1α (Fig. 8C) or HIF-2α (Fig. 8D) in hepatocytes cultured in room air.

Activation of Latent-TGF-β1 by Hypoxic Hepatocytes

Since hypoxia-induced EMT in hepatocytes required TGF-β signaling, we next investigated the mechanism by which hypoxia stimulated TGF-β signaling in hypoxic hepatocytes. Exposure of hepatocytes to hypoxia for 24 and 48 hours had no effect on mRNA levels of TGF-β1, TGF-β2, or TGF-β3 (Fig. 9). Exposure of hepatocytes to 1% oxygen for 24 hours increased the ratio of active TGF-β1 to total TGF-β1 in the culture medium, suggesting that hypoxic hepatocytes activate latent-TGF-β1 (Fig. 10A). Consistent with this, addition of latent TGF-β1 to hepatocytes cultured in 1% oxygen enhanced upregulation of FSP-1 and SNAIL, whereas addition of latent TGF-β1 to hepatocytes cultured in room air did not increase FSP-1 or SNAIL mRNA levels (Fig. 10B and 10C).

Reduced EMT in the Livers of HIF-1α-Deficient Mice after BDL

We demonstrated previously that liver fibrosis is reduced in HIF-1α-Deficient mice after BDL (4). To determine whether EMT was also reduced, BDLs were performed in Control mice, with normal levels of HIF-1α, and HIF-1α-Deficient mice. FSP-1 protein and mRNA levels were quantified as a biomarker of EMT. Minimal immunostaining for FSP-1 was observed in the livers of Control mice and HIF-1α-Deficient mice subjected to sham operation (Fig. 11A and 11B). After bile duct ligation, FSP-1 immunostaining was observed in periportal regions around proliferating bile ducts and within the hepatic parenchyma in periportal regions (Fig. 11C). In HIF-1α-Deficient mice, the extent of FSP-1 immunostaining was substantially reduced with minimal staining within the hepatic parenchyma and modest staining around proliferating bile ducts (Fig. 11D). Quantification of the area of FSP-1 immunostaining confirmed these results and demonstrated a significant increase in total FSP-1 immunostaining in the livers of Control mice after bile duct ligation, which was reduced in bile duct-ligated HIF-1α-Deficient mice (Fig. 12A). In addition, FSP-1 immunostaining was reduced both within peribiliary regions (i.e., FSP-1 immunostaining that occurred within 100 μm of CK-19 immunostaining) and nonperibiliary regions in HIF-1α-Deficient mice (Fig. 12A). Similar results were observed for FSP-1 mRNA levels (Fig. 12B).

Colocalization of FSP-1 with CK-19 and Albumin

In mice subjected to bile duct ligation for 10 days, numerous FSP-1 positive cells were observed adjacent to bile duct epithelial cells (Fig. 13A–C). No FSP-1 positive cells in this region also stained positive for CK-19 at this time point (Fig. 13C). Many FSP-1 positive cells were observed in the hepatic parenchyma away from proliferating bile ducts (Fig. 13D). Many of the FSP-1 positive cells in this region also stained positive for albumin (Fig. 13D–F).

Discussion

Regions of hypoxia develop in the liver during chronic injury (4). Furthermore, HIF-1α is activated in hepatocytes, and mice deficient in HIF-1α develop less liver fibrosis (4). These studies demonstrate that HIF-1α is essential for the development of liver fibrosis. The present studies indicate that HIF-1α may promote liver fibrosis in part by stimulating hepatocyte EMT.

As epithelial cells transdifferentiate into mesenchymal cells during EMT, levels of several transcription factors (e.g., Snail, Slug, TWIST), cytoskeletal proteins (e.g., α-SMA, vimentin), and signal transduction proteins (e.g., fibroblast-specific protein-1, (FSP-1)) are increased, and cytoskeletal proteins, such as F-actin, become reorganized into stress fibers (6, 13). In addition, transcriptional repressors, such as Snail, are increased and repress expression of epithelial genes, including E-cadherin, zona occludens-1 and others (6). In the present studies, exposure of primary mouse hepatocytes to chronic hypoxia stimulated F-actin polymerization, and increased expression of the mesenchymal cell markers α-SMA and vimentin (Fig. 1, 4, and 5). Furthermore, levels of two mediators of EMT, Snail and FSP-1, were increased in hypoxic hepatocytes, and levels of the epithelial proteins, E-cadherin and zona occludins-1, were decreased (Fig. 1, 2, and 4). These studies demonstrate for the first time that hypoxia stimulates hepatocyte EMT. It is unlikely that hepatic stellate cells contaminating the cultures were responsible for these changes as hepatic stellate cells made up less that 3% of the cells in the cultures, and exposure of purified hepatic stellate cells to hypoxia for 3 days did not increase levels of FSP-1, α-SMA, or Snail when compared to hepatic stellate cells cultured in room air (Fig. 3).

In renal epithelial cells, hypoxia-induced EMT depended in part on hypoxia-inducible factor signaling (5). We demonstrated previously that both HIF-1α and HIF-2α are activated in hypoxic hepatocytes (7). To determine whether these transcription factors are required for hypoxia-induced EMT in cultured hepatocytes, hepatocytes were isolated from HIF-1β-deficient mice. When HIF-1α and HIF-2α are activated in hypoxic cells, they translocate to the nucleus and heterodimerize with HIF-1β (14, 17). Heterodimerization with HIF-1β is required for upregulation of genes by HIF-1α and HIF-2α (14, 15). Therefore, loss of HIF-1β abrogates all HIF signaling in cells. In the present studies, deletion of HIF-1β completely prevented upregulation of EMT genes in hypoxic hepatocytes. Whether HIF-1β heterodimerized with HIF-1α and/or HIF-2α to stimulate hypoxia-induced EMT in these cells, however, is not known. Since mice deficient in HIF-1α developed less fibrosis and had reduced numbers of FSP-1 positive cells after BDL (Fig. 11 and 12), this would suggest that HIF-1α is important for this process (4). Studies have shown, however, that HIF-2α also regulates expression of genes in hepatocytes, and that HIF-2α can promote EMT in some cells types (7, 18, 19). Therefore, we cannot rule out the possibility that HIF-2α may also be important for this process. Further studies using HIF-1α and HIF-2α specific knockouts are needed to fully elucidate the role of each of these transcription factors in hypoxia-induced hepatocyte EMT.

In renal epithelial cells, hypoxia-induced EMT did not require TGF-β1 (5). Interestingly, in contrast to renal epithelial cells, hypoxia-induced EMT in hepatocytes was completely TGF-β-dependent (Fig. 7). This suggests that in hypoxic hepatocytes there is an interaction between HIFs and TGF-β signaling that leads to hepatocyte EMT. As mentioned, several studies have demonstrated that TGF-β1 stimulates hepatocyte EMT (3), and our studies suggest that under hypoxic conditions, HIFs in hepatocytes are able to facilitate TGF-β signaling. In some cell types, activation of HIFs by hypoxia requires TGF-β signaling, and TGF-β1 is able to activate HIFs independently of hypoxia (20, 21). Our studies demonstrate, however, that activation of HIFs in hepatocytes by hypoxia does not require TGF-β

signaling, and that TGF-β1 does not activate HIFs (Fig. 8). These results clearly demonstrate that TGF-β signaling is not required for HIF activation, and that TGF-β signaling is downstream of HIF activation in hypoxia-induced EMT.

Previous studies have demonstrated that HIFs regulate TGF-β3 in some cell types (22). In hepatocytes, however, hypoxia did not increase mRNA levels of any TGF-β, including TGF-β3 (Fig. 9). This suggested that hypoxia did not promote TGF-β-dependent EMT in hepatocytes by increasing TGF-β mRNA levels. Therefore, we next investigated whether hypoxia promoted activation of TGF-β1. TGF-βs are synthesized and secreted from cells in an inactive, latent form (23). Latent TGF-β requires proteolytic modification before it becomes active and initiates signaling in cells. Studies have demonstrated that hepatocytes in culture synthesize and release latent TGF-β1 (24). Furthermore, HIFs are known to regulate levels of several proteins that activate latent TGF-βs, such as urokinase plasminogen activator and matrix metalloproteinases (25, 26). Therefore, it is possible that when hepatocytes become hypoxic, they synthesize and secrete proteins that activate latent TGF-β, which stimulates hepatocyte EMT by an autocrine and paracrine mechanism. Consistent with this hypothesis, exposure of hepatocytes to hypoxia increased the ratio of active TGF-β1 to total TGF-β1 (Fig. 10A). Furthermore, addition of latent TGF-β1 to the hepatocyte cultures enhanced hypoxia-induced EMT (Fig. 10B–C). Collectively, these results demonstrate that hypoxic hepatocytes activate latent TGF-β1 and that this stimulates hepatocyte EMT. These observations are important as they may explain the mechanism by which chronic liver injury stimulates activation of latent TGF-β1 during the development of liver fibrosis. Regions of hypoxia develop in several models of liver fibrosis (4, 27, 28). Furthermore, TGF-β1 is an important stimulator of EMT, and stimulates hepatic stellate cell activation and collagen production (3, 29). Therefore, our results suggest that chronic liver injury, which causes persistent hypoxia in the liver, may drive fibrosis by stimulating hepatocytes to release a yet to be identified factor that activates latent TGF-β1. This process then stimulates EMT and activation of hepatic stellate cells resulting in fibrosis.

Consistent with a role of hypoxia and HIFs in hepatocyte EMT *in vitro*, HIF-1α was required for EMT *in vivo* (Fig. 11 and 12). Our results demonstrated that in bile duct-ligated mice, hepatocytes may contribute to the population of FSP-1 positive cells in the liver, as many of these cells also costained for albumin (Fig. 13). It is certainly possible that these cells accumulated albumin by phagocytosis, and were not derived from hepatocytes. Accordingly, lineage tracing studies, used previously to identify hepatocyte EMT in carbon tetrachloride-treated mice, are needed to confirm these results (3). Interestingly, FSP-1 expressing cells in peribiliary regions did not express CK-19, suggesting that these cells were not derived from bile duct epithelial cells. This is in contrast to studies in humans showing colocalization of FSP-1 with CK-19, a bile duct epithelial cell marker (2). It is possible that in mice, bile duct epithelial cells do not transdifferentiate into fibroblasts by EMT, or that in our studies, FSP-1 positive cells lost CK-19 expression by 10 days after bile duct ligation. Similar to hepatocytes, careful lineage tracing studies are needed to conclusively demonstrate whether bile duct epithelial cells transdifferentiate into fibroblasts by EMT *in vivo* during the development of fibrosis. Regardless of the cellular source of FSP-1 positive cells in the livers of bile duct-ligated mice, the numbers of FSP-1 positive cells were substantially reduced in both peribiliary and nonperibiliary regions of HIF-1α-Deficient mice (Fig. 11 and 12). Based upon our *in vitro* studies, it is possible that HIF-1α promoted activation of TGF-β1 which stimulated EMT both in peribiliary and nonperibiliary regions. Further studies are needed to evaluate this possibility.

Collectively, these results demonstrate for the first time that hypoxia is an important stimulus of hepatocyte EMT. Furthermore, these studies demonstrate that HIFs and TGF-β signaling contribute to the mechanism by which hypoxia stimulates hepatocyte EMT. A

greater understanding the mechanisms involved in hypoxia-induced EMT and the novel interaction between HIFs and TGF-β signaling, could lead to therapies aimed at reducing liver fibrosis in patients with this disease. Furthermore, it is possible that these studies may help to explain the mechanism by which hypoxia stimulates EMT in cancer—a process important for cancer metastasis.

Acknowledgments

This study was supported by National Institutes of Health grants DK073566 (B.L.C.) and COBRE (Center of Biomedical Research Excellence) P20 RR021940 as well as the Molecular Biology Core and the Histology Core supported by the COBRE grant. In addition, this work was supported by grant number P20 RR016475 from the National Center for Research Resources (NCRR), a component of the National Institutes of Health (NIH). The author thanks Dr. Frank J. Gonzalez at the National Cancer Institute for providing the HIF-1$\beta^{fl/fl}$-Mx-Cre+, HIF-1$\beta^{fl/fl}$-Mx-Cre−, HIF-1$\alpha^{fl/fl}$-Mx-Cre+, and HIF-1$\alpha^{fl/fl}$-Mx-Cre− mice for these studies. The author also thanks Callie Wentling, Bradly Sullivan, and Shan Bai for assistance with these studies.

References

1. Friedman SL. Mechanisms of hepatic fibrogenesis. Gastroenterology. 2008; 134(6):1655–69. [PubMed: 18471545]
2. Rygiel KA, Robertson H, Marshall HL, Pekalski M, Zhao L, Booth TA, et al. Epithelial-mesenchymal transition contributes to portal tract fibrogenesis during human chronic liver disease. Lab Invest. 2008; 88(2):112–23. [PubMed: 18059363]
3. Zeisberg M, Yang C, Martino M, Duncan MB, Rieder F, Tanjore H, et al. Fibroblasts derive from hepatocytes in liver fibrosis via epithelial to mesenchymal transition. J Biol Chem. 2007; 282(32): 23337–47. [PubMed: 17562716]
4. Moon JO, Welch TP, Gonzalez FJ, Copple BL. Reduced liver fibrosis in hypoxia-inducible factor-1alpha-deficient mice. Am J Physiol Gastrointest Liver Physiol. 2009; 296(3):G582–92. [PubMed: 19136383]
5. Higgins DF, Kimura K, Bernhardt WM, Shrimanker N, Akai Y, Hohenstein B, et al. Hypoxia promotes fibrogenesis in vivo via HIF-1 stimulation of epithelial-to-mesenchymal transition. J Clin Invest. 2007; 117(12):3810–20. [PubMed: 18037992]
6. Peinado H, Olmeda D, Cano A. Snail, Zeb and bHLH factors in tumour progression: an alliance against the epithelial phenotype? Nature reviews. 2007; 7(6):415–28.
7. Copple BL, Bustamante JJ, Welch TP, Kim ND, Moon JO. Hypoxia-inducible factor-dependent production of profibrotic mediators by hypoxic hepatocytes. Liver Int. 2009; 29(7):1010–21. [PubMed: 19302442]
8. Tomita S, Sinal CJ, Yim SH, Gonzalez FJ. Conditional disruption of the aryl hydrocarbon receptor nuclear translocator (Arnt) gene leads to loss of target gene induction by the aryl hydrocarbon receptor and hypoxia-inducible factor 1alpha. Molecular endocrinology (Baltimore, Md. 2000; 14(10):1674–81.
9. Tomita S, Ueno M, Sakamoto M, Kitahama Y, Ueki M, Maekawa N, et al. Defective brain development in mice lacking the Hif-1alpha gene in neural cells. Mol Cell Biol. 2003; 23(19):6739–49. [PubMed: 12972594]
10. Vrochides D, Papanikolaou V, Pertoft H, Antoniades a A, Heldin P. Biosynthesis and degradation of hyaluronan by nonparenchymal liver cells during liver regeneration. Hepatology. 1996; 23(6): 1650–5. [PubMed: 8675189]
11. Kim ND, Moon JO, Slitt a L, Copple BL. Early growth response factor-1 is critical for cholestatic liver injury. Toxicol Sci. 2006; 90(2):586–95. [PubMed: 16423862]
12. Copple BL, Roth RA, Ganey PE. Anticoagulation and inhibition of nitric oxide synthase influence hepatic hypoxia after monocrotaline exposure. Toxicology. 2006; 225(2–3):128–37. [PubMed: 16828949]
13. Masszi A, Di Ciano C, Sirokmany G, Arthur WT, Rotstein OD, Wang J, et al. Central role for Rho in TGF-beta1-induced alpha-smooth muscle actin expression during epithelialmesenchymal transition. Am J Physiol Renal Physiol. 2003; 284(5):F911–24. [PubMed: 12505862]

14. Jiang BH, Rue E, Wang GL, Roe R, Semenza GL. Dimerization, DNA binding, and transactivation properties of hypoxia-inducible factor 1. J Biol Chem. 1996; 271(30):17771–8. [PubMed: 8663540]
15. Wood SM, Gleadle JM, Pugh CW, Hankinson O, Ratcliffe PJ. The role of the aryl hydrocarbon receptor nuclear translocator (ARNT) in hypoxic induction of gene expression. Studies in ARNT-deficient cells. J Biol Chem. 1996; 271(25):15117–23. [PubMed: 8662957]
16. Inman GJ, Nicolas FJ, Callahan JF, Harling JD, Gaster LM, Reith a D, et al. SB-431542 is a potent and specific inhibitor of transforming growth factor-beta superfamily type I activin receptor-like kinase (ALK) receptors ALK4, ALK5, and ALK7. Molecular pharmacology. 2002; 62(1):65–74. [PubMed: 12065756]
17. Erbel PJ, Card PB, Karakuzu O, Bruick RK, Gardner KH. Structural basis for PAS domain heterodimerization in the basic helix--loop--helix-PAS transcription factor hypoxia-inducible factor. Proc Natl Acad Sci U S A. 2003; 100(26):15504–9. [PubMed: 14668441]
18. Kim WY, Perera S, Zhou B, Carretero J, Yeh JJ, Heathcote SA, et al. HIF2alpha cooperates with RAS to promote lung tumorigenesis in mice. J Clin Invest. 2009; 119(8):2160–70. [PubMed: 19662677]
19. Rankin EB, Biju MP, Liu Q, Unger TL, Rha J, Johnson RS, et al. Hypoxia-inducible factor-2 (HIF-2) regulates hepatic erythropoietin in vivo. J Clin Invest. 2007; 117(4):1068–77. [PubMed: 17404621]
20. Tabatabai G, Frank B, Mohle R, Weller M, Wick W. Irradiation and hypoxia promote homing of haematopoietic progenitor cells towards gliomas by TGF-beta-dependent HIF-1alpha-mediated induction of CXCL12. Brain. 2006; 129(Pt 9):2426–35. [PubMed: 16835250]
21. Mcmahon S, Charbonneau M, Grandmont S, Richard DE, Dubois CM. Transforming growth factor beta1 induces hypoxia-inducible factor-1 stabilization through selective inhibition of PHD2 expression. J Biol Chem. 2006; 281(34):24171–81. [PubMed: 16815840]
22. Nishi H, Nakada T, Hokamura M, Osakabe Y, Itokazu O, Huang LE, et al. Hypoxia-inducible factor-1 transactivates transforming growth factor-beta3 in trophoblast. Endocrinology. 2004; 145(9):4113–8. [PubMed: 15155569]
23. Annes JP, Munger JS, Rifkin DB. Making sense of latent TGFbeta activation. Journal of cell science. 2003; 116(Pt 2):217–24. [PubMed: 12482908]
24. Gressner OA, Lahme B, Siluschek M, Rehbein K, Herrmann J, Weiskirchen R, et al. Activation of TGF-beta within cultured hepatocytes and in liver injury leads to intracrine signaling with expression of connective tissue growth factor. Journal of cellular and molecular medicine. 2008; 12(6B):2717–30. [PubMed: 18266973]
25. Tacchini L, Matteucci E, De Ponti C, Desiderio MA. Hepatocyte growth factor signaling regulates transactivation of genes belonging to the plasminogen activation system via hypoxia inducible factor-1. Experimental cell research. 2003; 290(2):391–401. [PubMed: 14567996]
26. Shyu KG, Hsu FL, Wang MJ, Wang BW, Lin S. Hypoxia-inducible factor 1alpha regulates lung adenocarcinoma cell invasion. Experimental cell research. 2007; 313(6):1181–91. [PubMed: 17335808]
27. Rosmorduc O, Wendum D, Corpechot C, Galy B, Sebbagh N, Raleigh J, et al. Hepatocellular hypoxia-induced vascular endothelial growth factor expression and angiogenesis in experimental biliary cirrhosis. Am J Pathol. 1999; 155(4):1065–73. [PubMed: 10514389]
28. Corpechot C, Barbu V, Wendum D, Kinnman N, Rey C, Poupon R, et al. Hypoxia-induced VEGF and collagen I expressions are associated with angiogenesis and fibrogenesis in experimental cirrhosis. Hepatology. 2002; 35(5):1010–21. [PubMed: 11981751]
29. Hellerbrand C, Stefanovic B, Giordano F, Burchardt ER, Brenner DA. The role of TGFbeta1 in initiating hepatic stellate cell activation in vivo. J Hepatol. 1999; 30(1):77–87. [PubMed: 9927153]

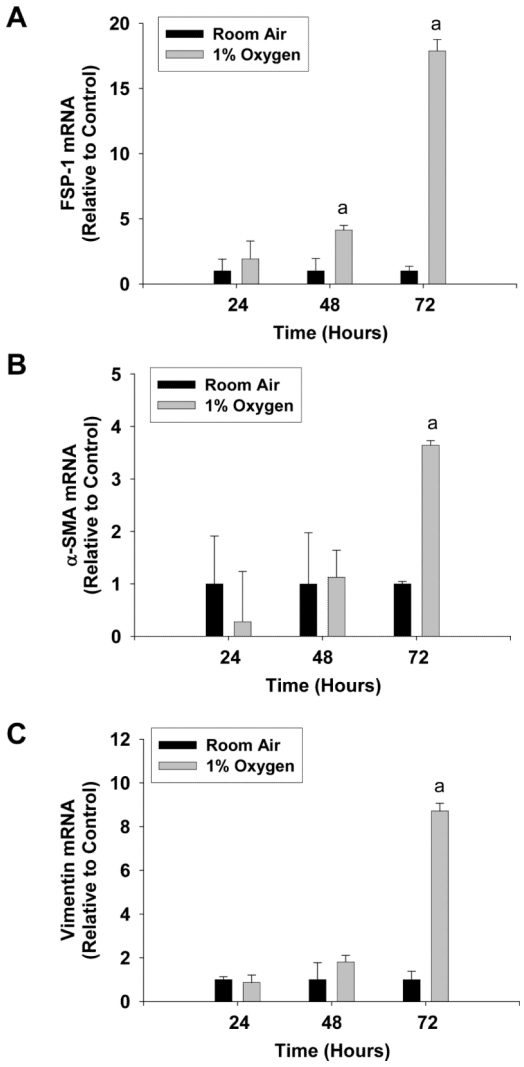

Fig. 1.

Hepatocytes were isolated from mice and exposed to room air or 1% oxygen for the indicated time. (A) FSP-1, (B) α-SMA, and (C) vimentin mRNA levels were measured by real-time PCR. [a]Significantly different from hepatocytes exposed to room air ($p<0.05$). Data are expressed as means ± SEM; n = 3.

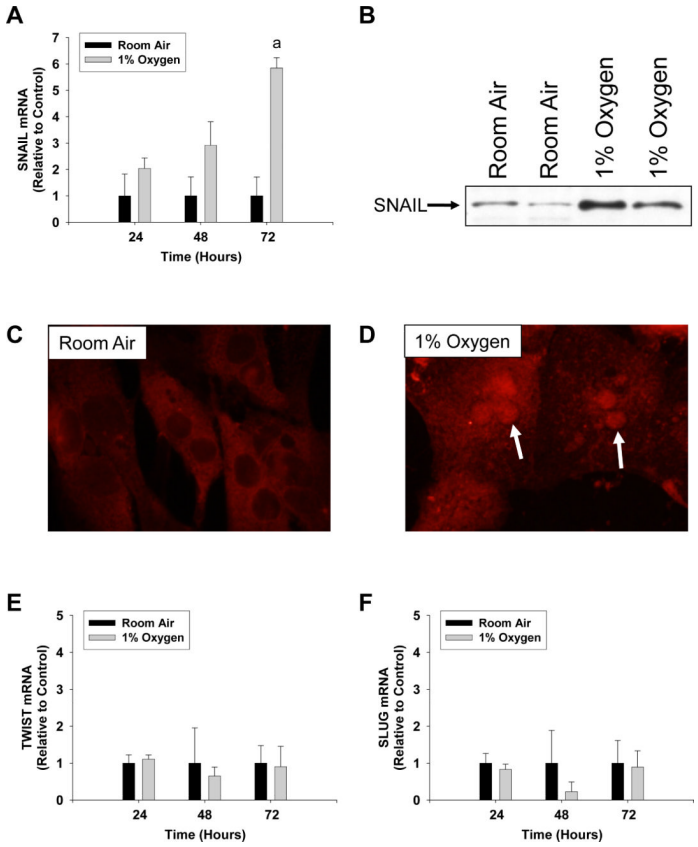

Fig. 2.

Hepatocytes were isolated from mice and exposed to room air or 1% oxygen for the indicated time (A, E, and F) or for 72 hours (B–D). (A) Snail mRNA levels were measured by real-time PCR. (B) Snail protein was measured in nuclear extracts by western blot. Snail protein was detected (red fluorescence) in hepatocytes exposed to (C) room air or (D) 1% oxygen by immunocytochemistry. Arrows indicate nuclear staining of Snail protein in hepatocytes exposed to 1% oxygen. (E) TWIST and (F) SLUG mRNA levels were measured by real-time PCR. [a]Significantly different from hepatocytes exposed to room air ($p<0.05$). Data are expressed as means ± SEM; n = 3.

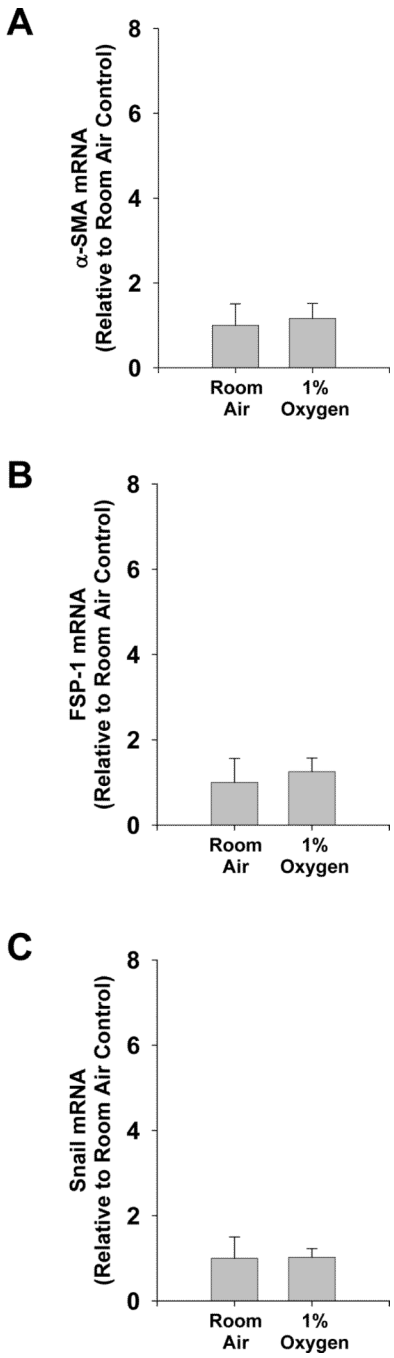

Fig. 3.

Hepatic stellate cells were isolated from mice and exposed to room air or 1% oxygen for 72 hours. (A) α-SMA, (B) FSP-1, and (C) Snail mRNA levels were measured by real-time PCR. mRNA levels are reported relative to room air. Data are expressed as means ± SEM; n = 3.

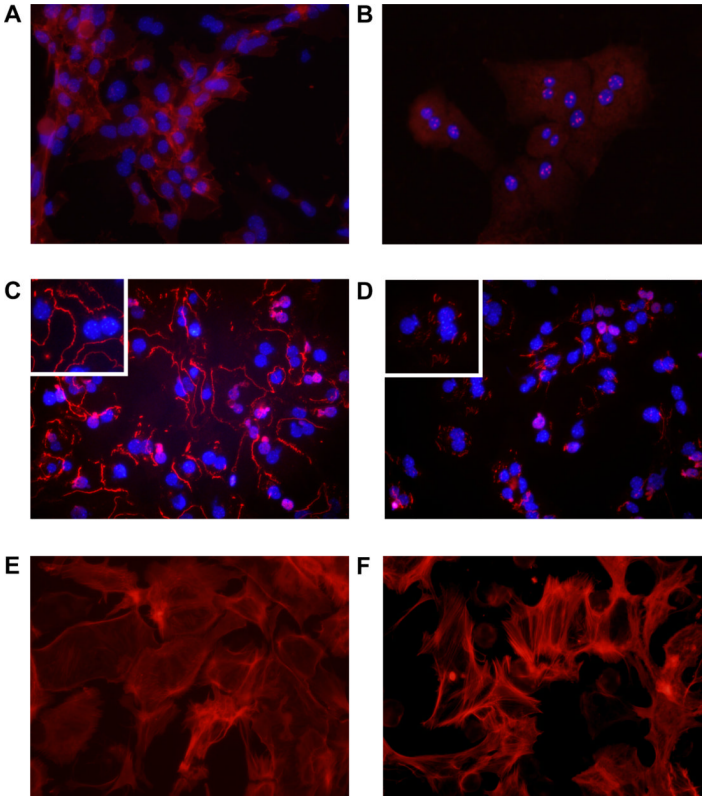

Fig. 4.

Hepatocytes were isolated from mice and exposed to room air (A, C, and E) or 1% oxygen (B, D, and F). (A and B) Three days later, E-cadherin was detected by immunocytochemistry (red fluorescence). (C and D) ZO-1 was detected by immunocytochemistry (red fluorescence). Higher power image is shown in the inset. In A–D the same cells were counterstained with DAPI (blue fluorescence) to identify the nuclei. (E and F) F-actin was detected by incubating with fluorescently-labeled phalloidin (red fluorescence).

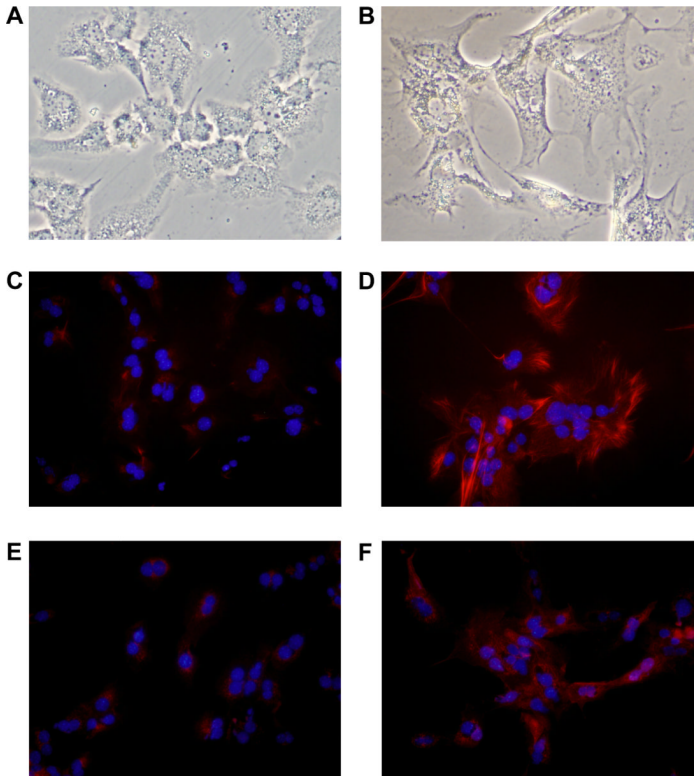

Fig. 5.

Hepatocytes were isolated from mice and exposed to room air (A, C, and E) or 1% oxygen (B, D, and F). (A and B) Light microscopic images of hepatocytes. Vimentin (C and D) and FSP-1 (E and F) were detected by immunocytochemistry (red fluorescence). In C–F the same cells were counterstained with DAPI (blue fluorescence) to identify the nuclei.

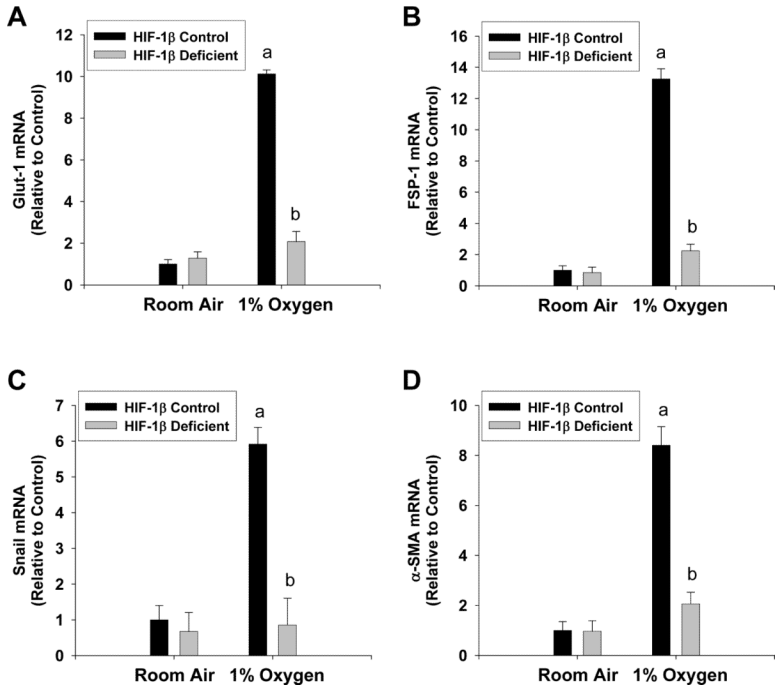

Fig. 6.

Hepatocytes were isolated from HIF-1β-Control and HIF-1β-Deficient mice, and exposed to room air or 1% oxygen. Seventy two hours later, (A) Glut-1, (B) FSP-1, (C) Snail, and (D) α-SMA mRNA levels were quantified by real-time PCR. [a]Significantly different from hepatocytes exposed to room air ($p<0.05$). [b]Significantly different from HIF-1β-Control hepatocytes exposed to the same concentration of oxygen ($p<0.05$).

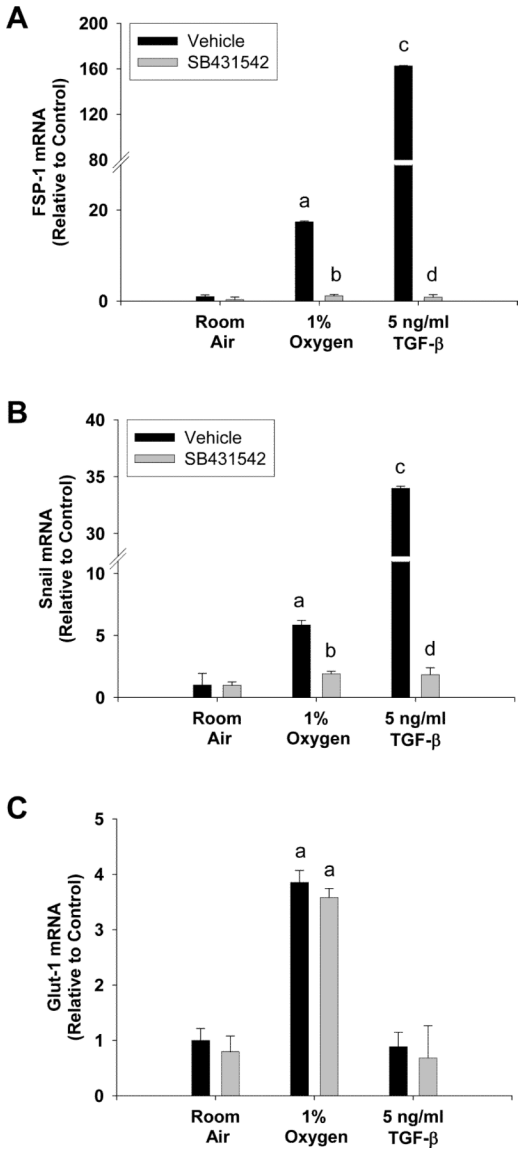

Fig. 7.

Hepatocytes were isolated from mice and treated with vehicle or SB-431542 for 30 minutes. The cells were then exposed to room air, 1% oxygen, or treated with TGF-β1. After 72 hours, (A) FSP-1, (B) Snail, and (C) Glut-1 mRNA levels were quantified by real-time PCR. [a]Significantly different from hepatocytes exposed to room air ($p<0.05$). [b]Significantly different from vehicle-treated hepatocytes exposed to the same concentration of oxygen ($p<0.05$). [c]Significantly different from hepatocytes exposed to vehicle and room air ($p<0.05$). [d]Significantly different from TGF-β1-treated hepatocytes ($p<0.05$). Data are expressed as means ± SEM; n = 3.

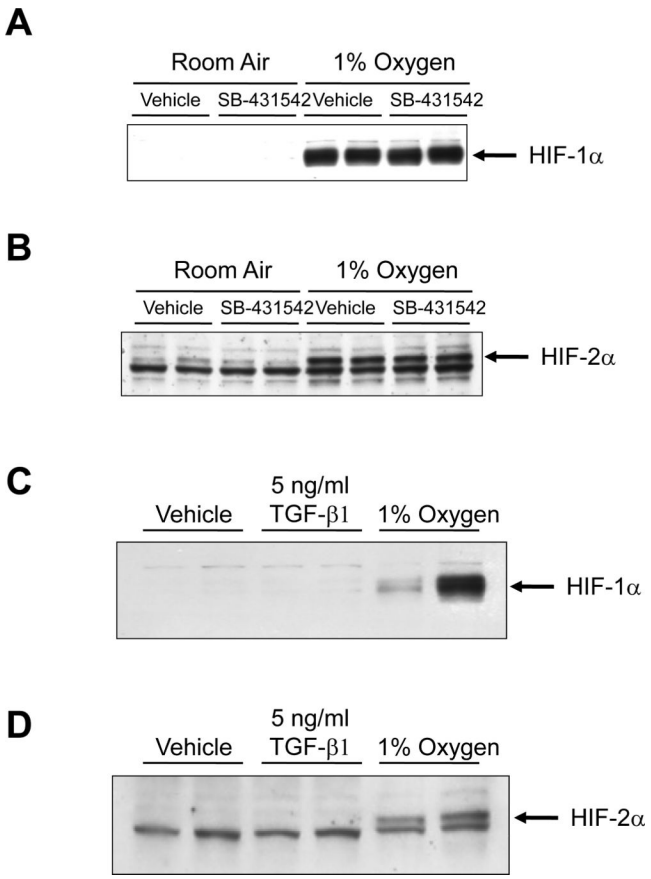

Fig. 8.

Hepatocytes were isolated from mice and treated with 10 μM SB-431542. Thirty minutes later, the cells were exposed to room air or 1% oxygen for 1 hour. (A) HIF-1α and (B) HIF-2α were detected by western blot. Representative of an n = 4. Hepatocytes were isolated from mice and treated with vehicle, 5 ng/ml TGF-β1, or exposed to 1% oxygen for 1 hour. (C) HIF-1α and (D) HIF-2α were detected by western blot. Representative of an n = 4.

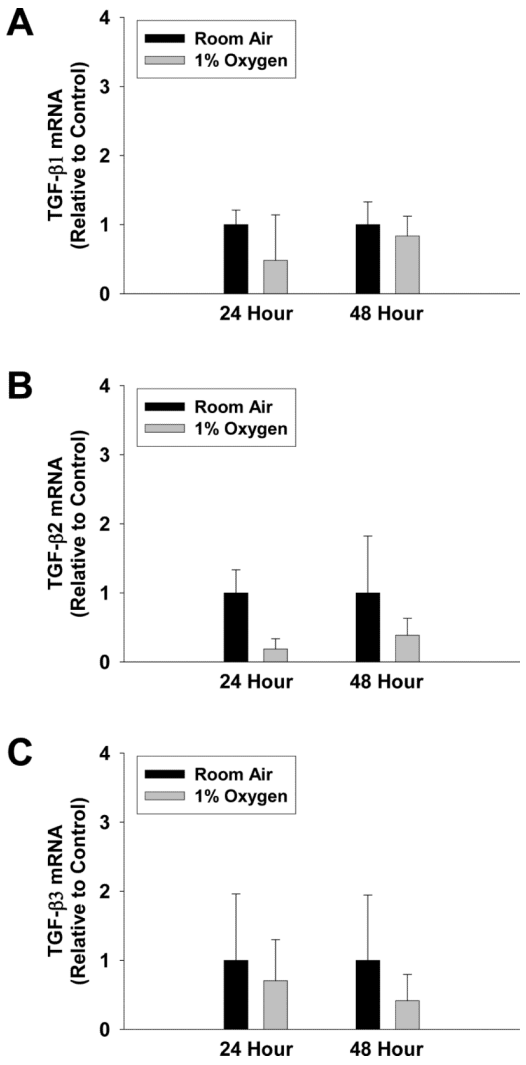

Fig. 9.

Hepatocytes were isolated from mice and exposed to room air or 1% oxygen for 24 or 48 hours. (A) TGF-β1, (B) TGF-β2, and (C) TGF-β3 mRNA levels were quantified by real-time PCR. Data are expressed as means ± SEM; n = 3.

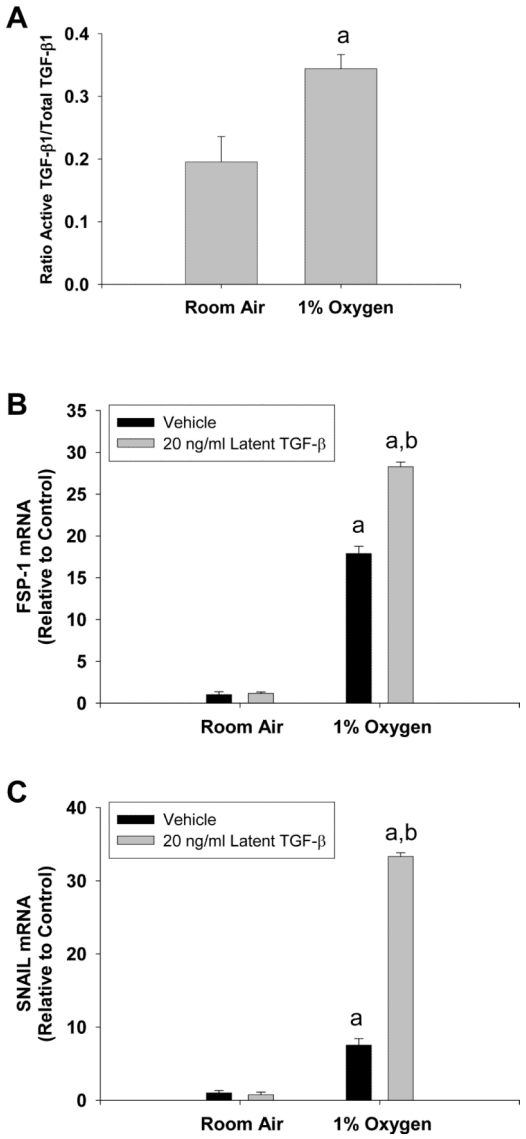

Fig. 10.

Hepatocytes were exposed to room air or 1% oxygen for 24 hours. Active and total TGF-β1 were quantified by ELISA. [a]Significantly different from hepatocytes exposed to room air ($p<0.05$). Data are expressed as means ± SEM; n = 3. Hepatocytes were treated with vehicle or 20 ng/ml latent TGF-β1 followed by exposure to room air or 1% oxygen. 72 hours later, FSP-1 and Snail mRNA levels were quantified. [a]Significantly different from hepatocytes exposed to room air ($p<0.05$). [b]Significantly different from hepatocytes exposed to vehicle and 1% oxygen ($p<0.05$). Data are expressed as means ± SEM; n = 3.

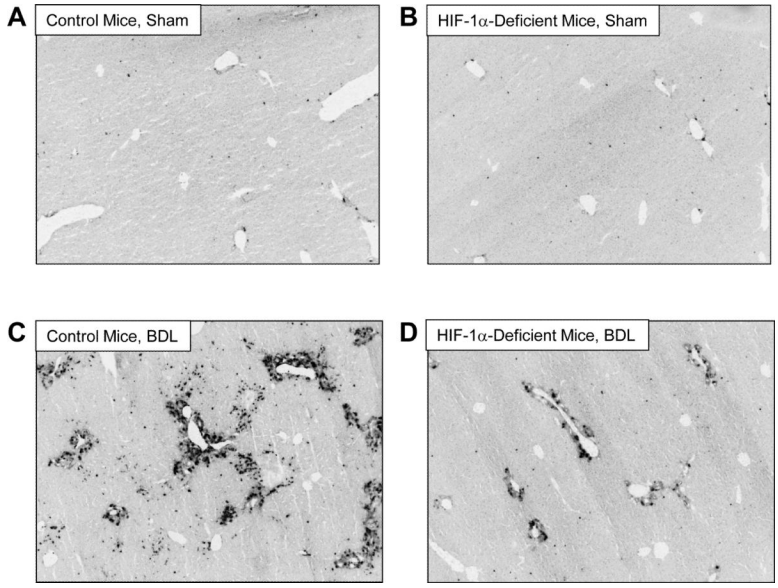

Fig. 11.

Control mice and HIF-1α-Deficient mice were subjected to bile duct ligation or sham operation. Fourteen days later, FSP-1 was detected in the liver by immunohistochemistry. Representative photomicrograph of a section of liver from a (A) Control mouse sham operation, (B) HIF-1α-Deficient mouse sham operation, (C) Control mouse bile duct ligation, and (D) HIF-1α-Deficient mouse bile duct ligation stained for FSP-1. Positive staining for collagen appears dark grey in the photomicrographs.

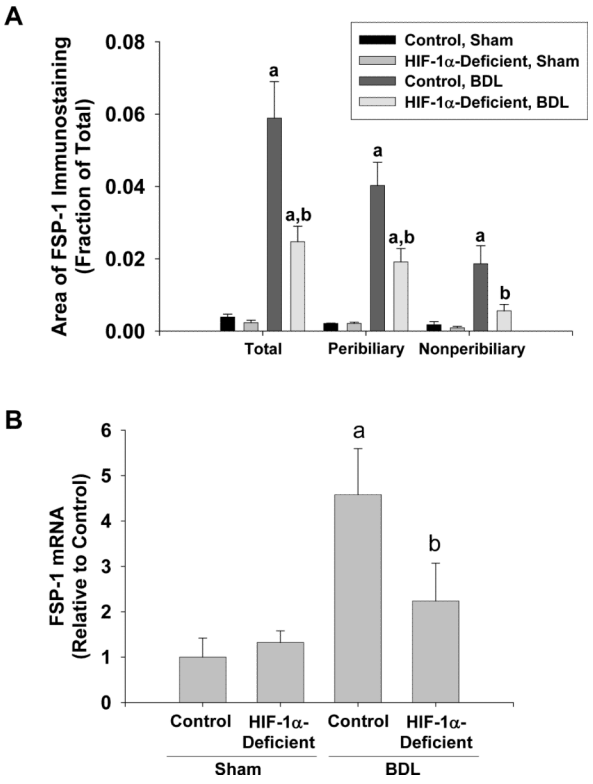

Fig. 12.

Control mice and HIF-1α-Deficient mice were subjected to bile duct ligation or sham operation. Fourteen days later, FSP-1 was detected in the liver by immunohistochemistry. (A) Total, peribiliary, and nonperibiliary area of FSP-1 immunostaining was analyzed morphometrically. (B) FSP-1 mRNA levels were quantified in the liver by real-time PCR. [a]Significantly different from sham-operated mice ($p<0.05$). [b]Significantly different from Control mice subjected to bile duct ligation ($p<0.05$). Data are expressed as means ± SEM; n = 6.

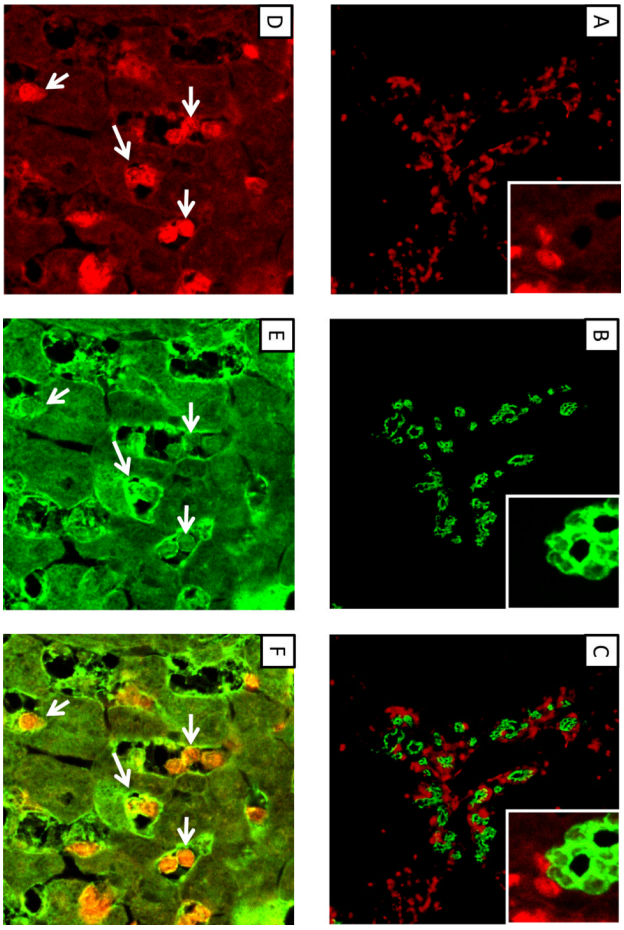

Fig. 13.

Wild-type mice were subjected to bile duct ligation. Ten days later, FSP-1 (A and D, red staining), CK19 (B, green staining), and albumin (E, green staining) were detected by immunohistochemistry. (C) FSP-1 immunostaining (red) in A and CK19 immunostaining (green) in B were overlaid to detect colocalization. Higher power image in A, B, and C shown in inset. (F) FSP-1 immunostaining (red) in D and albumin immunostaining (green) in E were overlaid to detect colocalization. Arrows indicate FSP-1 positive cells that also stain positive for albumin.